

Dispersion studies of La substitution on dielectric and ferroelectric properties of multiferroic BiFeO₃ ceramic

K. Sen ^{*}, K. Singh, Ashish Gautam, M. Singh

Department of Physics, Himachal Pradesh University, Shimla-171005, India

Received 19 April 2011; received in revised form 18 June 2011; accepted 28 June 2011

Available online 5th July 2011

Abstract

Lanthanum La-substituted multiferroic Bi_{1-x}La_xFeO₃ ceramics with $x = 0.0, 0.05, 0.10, 0.15, 0.20$ and 0.25 have been prepared by solution combustion method. The effect of La substitution for the dispersion studies on dielectric and ferroelectric properties of Bi_{1-x}La_xFeO₃ samples have been studied by performing x-ray diffraction (XRD), transmission electron microscopy (TEM), scanning electron microscopy (SEM), density, dc resistivity and dielectric measurements as well as characterizing the polarization-field hysteresis loop. The results of prepared samples are compared with those of bismuth ferrite (BiFeO₃). In the measuring frequency of 10 KHz to 1 MHz, the dielectric constants and dielectric losses for samples $x = 0.20, 0.25$ are almost stable and exhibited lowest dielectric loss close to 0.1. The resistivity of Bi_{1-x}La_xFeO₃ samples reaches a maximum value of 10⁹ ohm-cm, which is about three times higher than that for pure BiFeO₃. The results also show that stabilization of crystal structure and nonuniformity in spin cycloid structure by La substitution enhances the resistivity, dielectric and ferroelectric properties. Furthermore, the substitution of rare earth La for Bi helps to eliminate the impurity phase in BiFeO₃ ceramic.

© 2011 Elsevier Ltd and Techna Group S.r.l. All rights reserved.

Keywords: A. Calcination; B. Porosity; C. Dielectric Properties; E. Sensors

1. Introduction

Multiferroic materials possess the properties of ferroelectricity, ferromagnetism and even ferroelastic simultaneously due to the coupling between ferroelectric and ferromagnetic orders within one phase. Multiferroic materials have attracted much attention in recent years [1,2], because of their potential for new device applications [3–5]. The main multiferroic oxides studied so far include BiFeO₃ (BFO), BiMnO₃ and ReMnO₃ (Re = Y, Ho–Lu). Among them, BFO has a high Curie temperature ($T_C \sim 830$ °C) and a high Neel temperature ($T_N \sim 370$ °C), and it shows a rhombohedrally distorted perovskite crystal structure with space group R3c and G-type antiferromagnetism at room temperature [6]. The ferroelectric mechanism in BFO is conditioned by the stereochemically active 6s² lone pair of Bi³⁺ while the weak ferromagnetic property is caused by residual moment from the canted Fe³⁺ spin structure [7]. The coupling effect between magnetic and

electric behaviors occurs through the lattice distortion of BFO when an electric field or a magnetic field is applied [8], which offers new routes to the design and application of information storages, spintronics, sensors, etc. [9,10]. However, in the processing of BiFeO₃, the valence fluctuation of iron ions (i.e., from 3+ to 2+) leads to large leakage and impurities in BiFeO₃ bulk, which enshrouds intrinsic properties of BiFeO₃. Recently, some sintering methods such as rapid liquid sintering [11] and spark plasma sintering [12] were used to restrain the appearance of impurities phases. Furthermore, it has been also found that, some additives such as, La, Nd, and Tb [13–16] facilitated the formation of the single phase. Moreover, the relatively high conductivity in these kinds of materials becomes an obstacle for the application of higher electric fields, especially at high temperatures. Srinivas et al. [17] synthesized rare earth substituted bismuth iron titanate and enhanced the resistivity and magnetoelectric effect. Therefore, it is expected that the resistivity of BiFeO₃ can be controlled by donor doping and thus also the dielectric, ferroelectric properties of multiferroic ceramics. Wang et al. [18] observed an improvement in the dielectric properties of BiFeO₃ on substituting La at the Bi site and Ga at the Fe site, and making its composite with

^{*} Corresponding author. Tel.: +91 0177 2830950; fax: +91 0177 2830775.

E-mail address: sen.728@gmail.com (K. Sen).

43 mol% of PbTiO_3 . The room temperature dielectric constant was found to be 1800 with low loss tangent of 0.024. In this paper, we report the dispersion studies of La substitution (5–25 mol% at the Bi site) on dielectric and ferroelectric properties of BiFeO_3 ceramic [i.e., $\text{Bi}_{1-x}\text{La}_x\text{FeO}_3$ (BFOL)].

2. Experimental

Ceramic samples of $\text{Bi}_{1-x}\text{La}_x\text{FeO}_3$, $x = 0.0, 0.05, 0.10, 0.15, 0.20$ and 0.25 were prepared using a solution combustion method by mixing appropriate amounts of $\text{Fe}(\text{NO}_3)_3 \cdot 9\text{H}_2\text{O}$, $\text{Bi}(\text{NO}_3)_3 \cdot 5\text{H}_2\text{O}$, $\text{La}(\text{NO}_3)_3 \cdot 6\text{H}_2\text{O}$ and L-alanine were first dissolved in 2-methoxyethanol for 45 min by means of ultrasonic cleaner. 5 mol% excess bismuth nitrate was added to compensate the Bi loss during sintering. A clear solution was obtained by the constant stirring for 3 h. Solution was then heated at magnetic stirrer heater at 80°C with constant stirring till auto-combustion took place. The prepared powder was grounded and calcined at 400°C for 2 h, at 600°C for 1 h and at 855°C for 30 min. The obtained powders were milled again, and then pressed into 1 mm-thick pellets of 15 mm in diameter. The pellets were sintered at 855°C rapidly for 30 min. For resistivity, dielectric and ferroelectric measurements, both surfaces of pellets were polished with silver paste to make electrodes. X-ray diffraction data for powder sample was collected using a PANalytical XPERT-PRO diffractometer with $\text{Cu K}\alpha$ radiation at a step of 0.02 in the range $2\theta = 20^\circ$ – 60° . TEM measurements of powder samples were carried out by Hitachi H7500 with resolving power 2Å . The scanning electron micrographs (SEM) of the pellet samples were taken to study the grain size and size distributions. The density of pellet samples were determined using the immersion technique. Electrical resistivity measurements were carried out using Keithley electrometer for measuring dc resistivity. Room temperature ferroelectric measurements were carried out using loop tracer at frequency of 50 Hz. Dielectric constant and dielectric loss were performed using a precision impedance analyzer Wayne Kerr 6500B over the frequency range from 10 KHz to 1 MHz.

3. Results and discussion

Fig. 1 shows the XRD pattern of the $\text{Bi}_{1-x}\text{La}_x\text{FeO}_3$ ceramic powder samples with $x = 0.0, 0.05, 0.10, 0.15, 0.20$, and 0.25 . It can be seen that the ceramics show single-phase characteristics. Though all the diffraction peaks were well identified, few low intensity peaks were observed at $2\theta \sim 27^\circ$ – 28° in case of BiFeO_3 ceramic [19]. X-ray diffraction pattern indicates the presence of bismuth ferrite impurity phase $\text{Bi}_2\text{Fe}_4\text{O}_9$ (* marked) in $\text{Bi}_{1-x}\text{La}_x\text{FeO}_3$ samples with $x = 0.0$ (BiFeO_3). Because of the formation kinetics, a mixture of BiFeO_3 as a major phase along with other impurity phases was always obtained during synthesis [20,21]. There has been no trace of La_2O_3 in the samples with x upto 0.25. This indicates that the La^{3+} ions have been incorporated in the BiFeO_3 structure. The lattice constants of $\text{Bi}_{1-x}\text{La}_x\text{FeO}_3$ ceramic are: for $x = 0.0$, $a = 3.933\text{Å}$, for $x = 0.05$, $a = 3.932\text{Å}$, for $x = 0.10$, $a = 3.929\text{Å}$, for $x = 0.15$, $a = 3.922\text{Å}$,

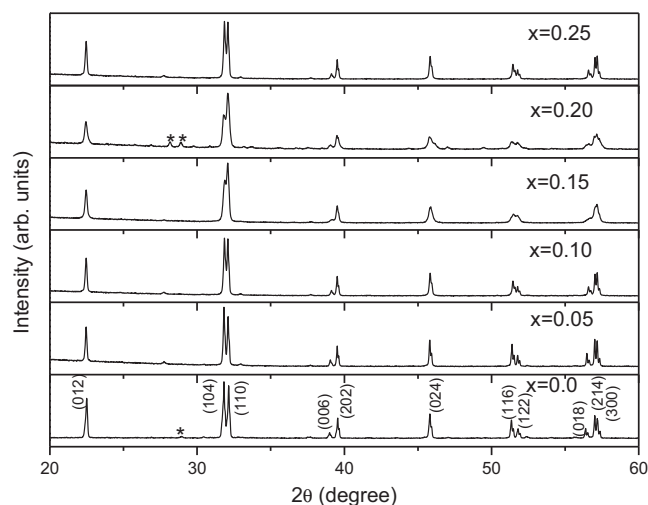


Fig. 1. X-ray diffraction patterns of $\text{Bi}_{1-x}\text{La}_x\text{FeO}_3$ ceramics powder sample (* marked $\text{Bi}_2\text{Fe}_4\text{O}_9$ impurity phase).

for $x = 0.20$, $a = 3.922\text{Å}$ and for $x = 0.25$, $a = 3.929\text{Å}$. The lattice constants change slightly linearly with the La content, which can be attributed to the slightly change ionic radius of La^{3+} (1.032Å) than that of Bi^{3+} (1.030Å) ions. It was reported that doping rare earth La could eliminate the impurity phase $\text{Bi}_2\text{Fe}_4\text{O}_9$ in BiFeO_3 [17]. It should be noted that the diffraction intensity from the impurity in the sample with $x = 0.05, 0.10, 0.20$ and 0.25 is weaker than in the undoped one, while no observable impurity peaks are observed in the XRD pattern of the samples with $x = 0.15$. This means that doping with La hinders the formation of a second phase. One feature that should be noted in Fig. 1 is that with increasing La composition, the intensity of some diffraction peaks, e.g. (0 0 6) and (0 1 8), becomes weak and tends to disappear near $x = 0.15$. XRD pattern of the $\text{Bi}_{1-x}\text{La}_x\text{FeO}_3$ ceramic powder samples are well consistent with Das et al. [19]. The particle size was calculated from XRD peak broadening using Scherrer formula [22]. The average particles size for $\text{Bi}_{1-x}\text{La}_x\text{FeO}_3$ ceramics powder is 20.6 nm, 22.4 nm, 22.8 nm, 23.2 nm, 23.6 nm and 24.0 nm for $x = 0.0, 0.05, 0.10, 0.15, 0.20, 0.25$ samples, respectively.

Fig. 2 shows the TEM micrographs for powder sample with composition $x = 0.05$, the morphology of the particles seemed to be approximately spherical. The values of the particle size as obtained from TEM images are in good agreement with the one, calculated from XRD patterns.

Fig. 3 shows the scanning electron micrographs of $\text{Bi}_{0.95}\text{La}_{0.05}\text{FeO}_3$ ceramic. The average grain size of the pellet samples is very much similar, and in the range of 1–10 μm . The density of pellet samples are 7.403 g/cm^3 , 9.156 g/cm^3 , 11.412 g/cm^3 , 8.196 g/cm^3 , 6.353 g/cm^3 , 6.025 g/cm^3 , respectively ($x = 0.0, 0.05, 0.10, 0.15, 0.20, 0.25$), with porosity of nearly 99.9%. However, it can be noticed that with a small lanthanum concentration (5–10 mol%), the density of sample (i.e., less voids) increases. The microstructures and absence of secondary phases on La substitution in BFO are some of the main reasons for enhanced resistivity and dielectric properties of BFOL. Smaller grain size results in larger number of grain

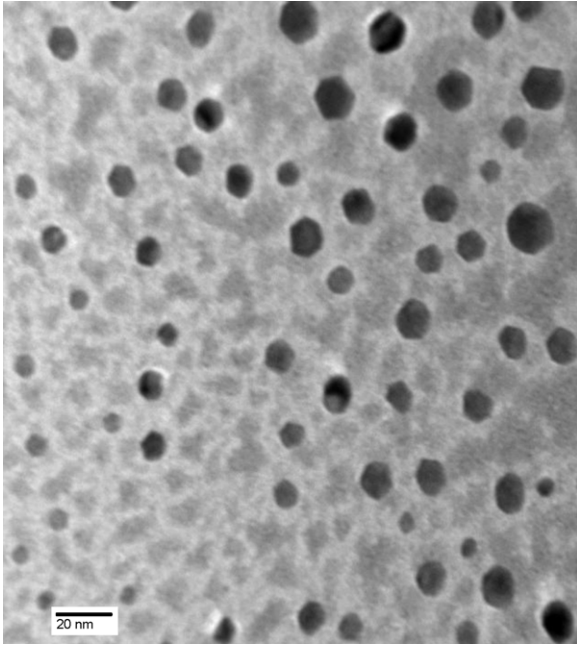


Fig. 2. TEM micrographs of $\text{Bi}_{0.95}\text{La}_{0.05}\text{FeO}_3$ ceramic powder sample sintered at 855 °C.

boundaries, which act as scattering centre for the flow of electrons and therefore increasing the resistivity which is shown in Fig. 4 at room temperature.

Fig. 5 shows the dielectric constant of $\text{Bi}_{1-x}\text{La}_x\text{FeO}_3$ samples at room temperature as a function of frequency. The dielectric constant at low frequency level increases for content $x = 0.05, 0.10, 0.15$ and with the increase of frequency it decreases as compared with pure BiFeO_3 , which is consistent with a combined response of orientational relaxation of dipoles

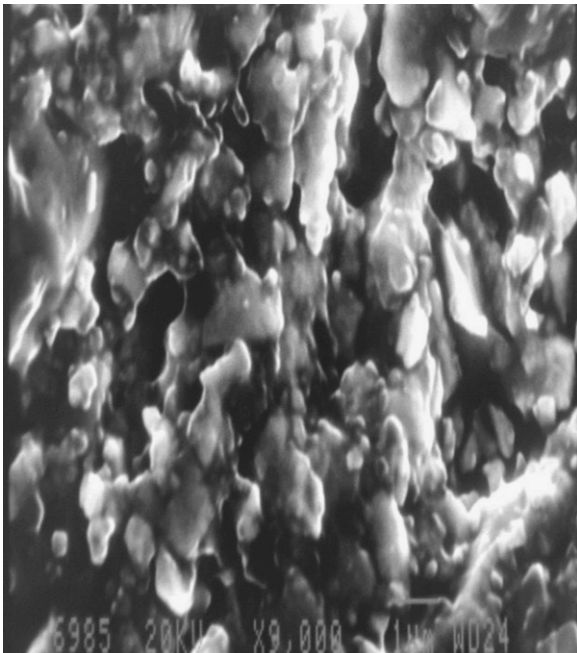


Fig. 3. SEM micrographs of $\text{Bi}_{0.95}\text{La}_{0.05}\text{FeO}_3$ ceramic pellet sample sintered at 855 °C.

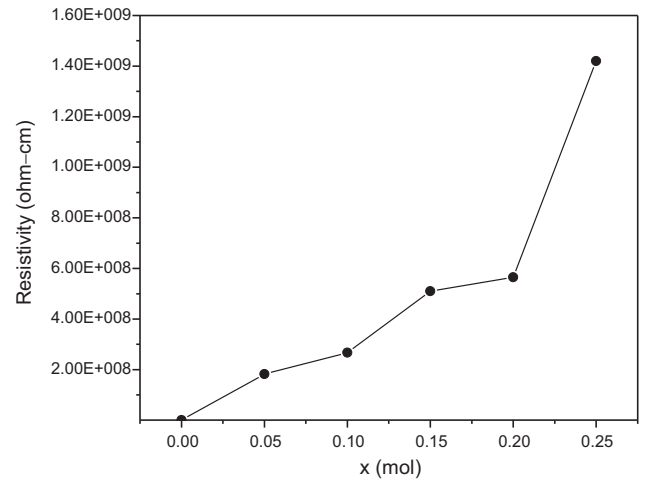


Fig. 4. Resistivity of $\text{Bi}_{1-x}\text{La}_x\text{FeO}_3$ ceramics sample with La content, x at room temperature.

and the conduction of charge carriers [23]. For $x = 0.20$ and 0.25 , the dielectric constant is almost constant in the low and high frequency region. The variation of dielectric constant reveals the dispersion due to Maxwell [24] interfacial polarization and is in agreement with Koops phenomenological theory [25]. The initial slow decrease in the dielectric constant as predicted by Koops model has not been observed in the present study. This is because the lowest frequency employed in the present investigations is too high to observe the initial slow variation of dielectric constant with frequency. The physical reason for the dispersion of dielectric constant can be understood on the basis of hopping of electrons between $\text{Fe}^{2+} \rightarrow \text{Fe}^{3+}$ pairs of ions. The applied electric field displaces the electrons slightly from their equilibrium positions, thus producing polarization. The dielectric constant value of the $\text{Bi}_{1-x}\text{La}_x\text{FeO}_3$ ceramics was higher than those of the reported pure BiFeO_3 ceramics [26,27].

Fig. 6 shows the dielectric loss of $\text{Bi}_{1-x}\text{La}_x\text{FeO}_3$ samples at room temperature as a function of frequency. Similar to the dielectric constant, the dielectric loss also decreases smoothly

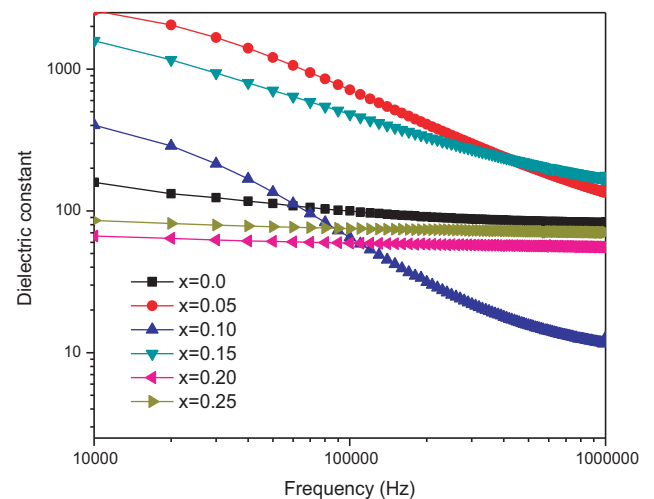


Fig. 5. Dielectric constant of $\text{Bi}_{1-x}\text{La}_x\text{FeO}_3$ samples at room temperature as a function of frequency with different La content, x .

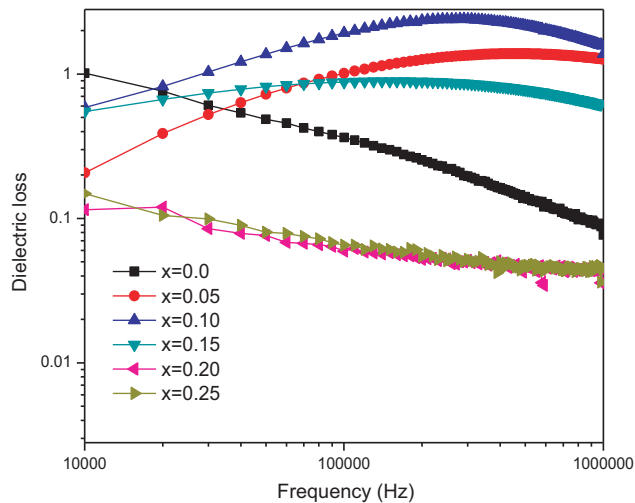


Fig. 6. Dielectric loss of $\text{Bi}_{1-x}\text{La}_x\text{FeO}_3$ samples at room temperature as a function of frequency with different La content, x .

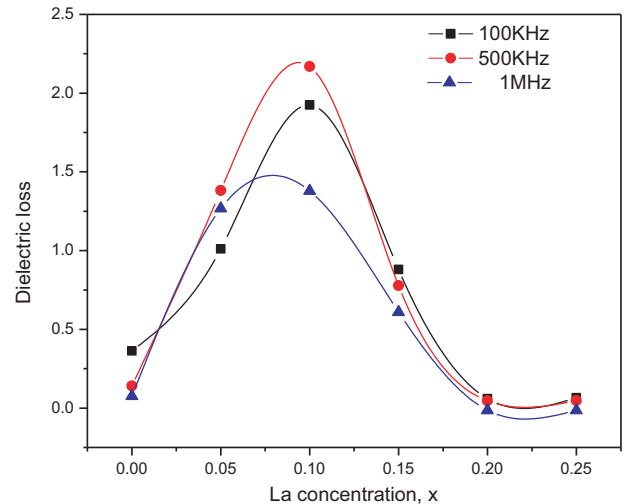


Fig. 8. Dielectric loss of $\text{Bi}_{1-x}\text{La}_x\text{FeO}_3$ ceramic samples measured at selected frequency.

with increasing frequency, which is consistent with the results reported in Ref. [28]. However, the dip in the dielectric loss reported in Ref. [28] is not present here. The La doped samples with $x = 0.20$ and 0.25 have less dielectric loss than that of pure BFO. Furthermore, it was also observed that both dielectric constant and dielectric loss for $x = 0.20$ and 0.25 samples are rather stable over the entire frequency range investigated, particularly in the frequency range between 10 KHz and 1 MHz.

To further investigate the effect of La substitution on the dielectric property of these samples, the dielectric constant and dielectric loss at selected frequencies have been plotted as a function of La concentration, x (Figs. 7 and 8). No systematic increase in dielectric constant with increase in the concentration of La is observed. It is striking to see that the dielectric constant increases dramatically with small amount of La substitution (Fig. 7), the dielectric constant measured at 100 KHz reaches a maximum value of 700 when $x = 0.05$, seven times as big as that for pure BiFeO_3 . Further increasing in

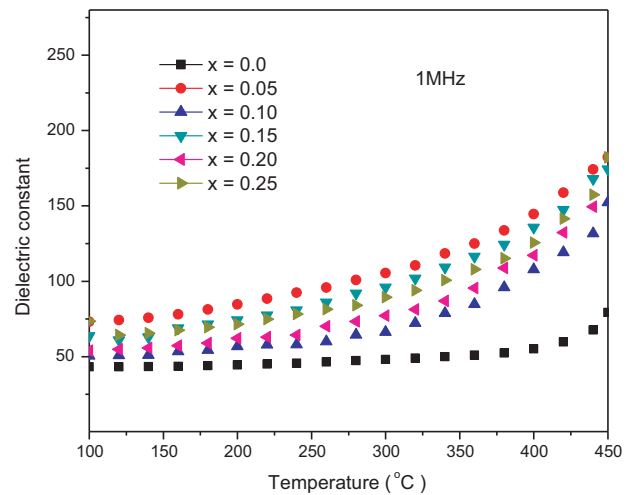


Fig. 9. Temperature dependence of the dielectric constant of $\text{Bi}_{1-x}\text{La}_x\text{FeO}_3$ ceramic samples at 1 MHz.

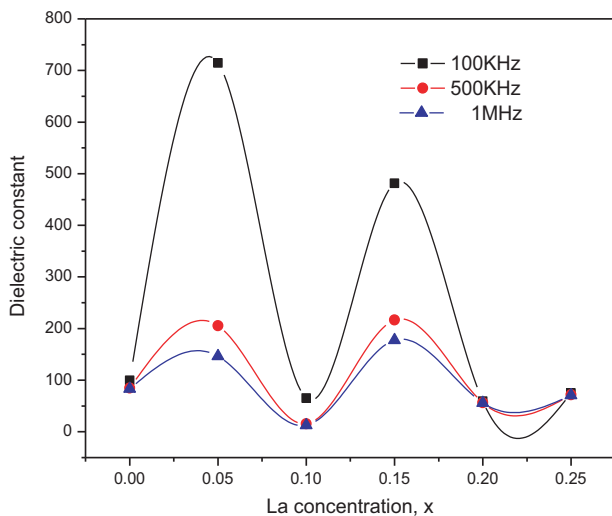


Fig. 7. Dielectric constant of $\text{Bi}_{1-x}\text{La}_x\text{FeO}_3$ ceramic samples measured at selected frequency.

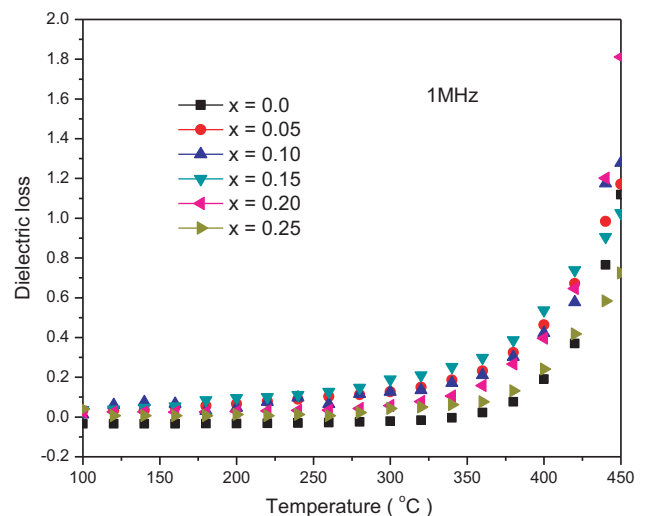


Fig. 10. Temperature dependence of the dielectric loss of $\text{Bi}_{1-x}\text{La}_x\text{FeO}_3$ ceramic samples at 1 MHz.

the La content ($x = 0.10$), reduces the value of the dielectric constant back to the level for pure BiFeO_3 . Another maximum of dielectric constant appears at $x = 0.15$ and more La doping ($x = 0.20, x = 0.25$) leads to another drop in dielectric constant (Fig. 7). This dielectric behavior of $\text{Bi}_{1-x}\text{La}_x\text{FeO}_3$ ceramics might be understood in terms of oxygen vacancy and the displacement of Fe^{3+} ions. There are always some oxygen vacancies in pure BiFeO_3 , which results in relatively high conductivity and small dielectric constant [29]. Substitution of small amount ($x = 0.0–0.05$) of more stable La^{3+} for Bi^{3+} would

stabilize the perovskite structure of BiFeO_3 and hence reduce the number of oxygen vacancies and subsequently increases the dielectric constant. Further increase in La content ($x = 0.05–0.10$) would result in a unit cell volume contraction, because ionic radius of La^{3+} is slightly changed than that of Bi^{3+} . The free volume available for the displacement of Fe^{3+} ions in the Fe–O oxygen octahedral becomes smaller and this would lead to a decrease in dielectric polarization. As La content x is greater than 0.10 but less than 0.15, the mismatch between BiFeO_3 and LaFeO_3 lattice constant prevents the grains from

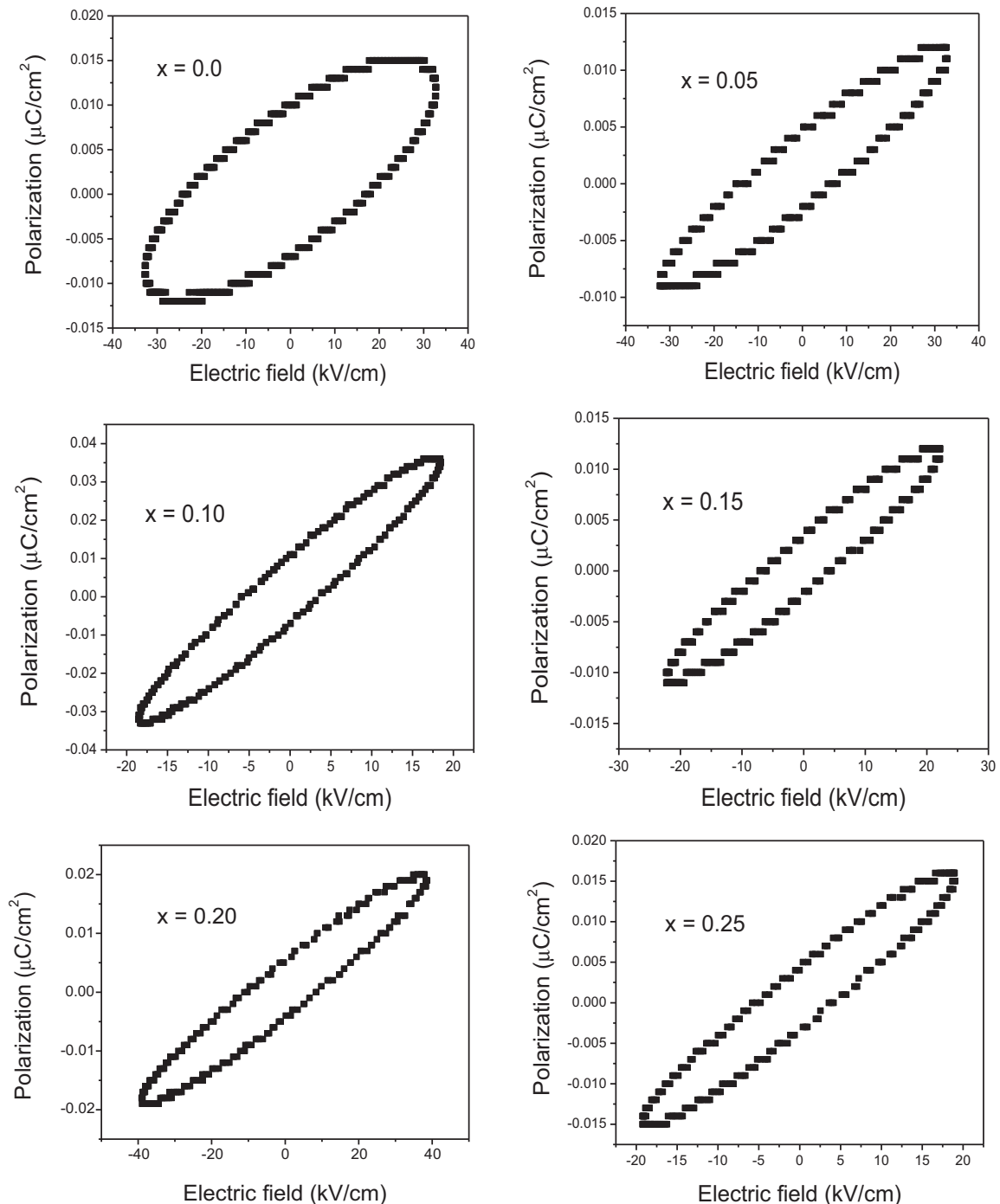


Fig. 11. Ferroelectric (P–E) loops for $\text{Bi}_{1-x}\text{La}_x\text{FeO}_3$ ceramics sample at room temperature.

growing big, which introduces more grain boundaries. As a result, the dielectric constant would increase again (see the peak at $x = 0.15$ in Fig. 7). A saturation level of La content for forming a solid solution is gradually approached when x is increased from 0.15 to 0.25. At this stage, the sample might be a composite of La_2O_3 and ferroelectric BiFeO_3 , with a smaller dielectric constant ($x = 0.20, 0.25$ in Fig. 7). Another feature of $\text{Bi}_{1-x}\text{La}_x\text{FeO}_3$ ceramics observed in Fig. 7 is that the frequency dependence of the dielectric constant of samples with La content $x = 0.05$ and 0.15 is remarkably enhanced and the dielectric constant of samples with $x = 0.10, 0.20$ and 0.25 is almost independent of frequency. This observation may have important ramifications for the practical application of this material. The effect of La substitution on the dielectric loss angle is shown in Fig. 8. The dielectric loss in $\text{Bi}_{1-x}\text{La}_x\text{FeO}_3$ ceramics increases dramatically with a small amount of La substitution ($x = 0.0–0.10$) and reaches a maxima at $x = 0.10$. Further increasing in the La content ($x = 0.15–0.25$), reduces the value of the dielectric loss back to the level for pure BiFeO_3 and minimum dielectric loss is reached when $x = 0.20$ and 0.25 .

Figs. 9 and 10 show the temperature dependence of the dielectric constant and dielectric loss for the samples $x = 0.0, 0.05, 0.10, 0.15, 0.20$ and 0.25 at 1 MHz. The values of dielectric constant and dielectric loss increase slowly with a rise in temperature. However, a sharp increase in dielectric constant and dielectric loss started from $350\text{ }^\circ\text{C}$ to $400\text{ }^\circ\text{C}$. But in the said temperature range, we could not find any dielectric anomaly or phase transition for any composition of $\text{Bi}_{1-x}\text{La}_x\text{FeO}_3$ ceramics.

Fig. 11 shows the ferroelectric hysteresis loops for all samples at room temperature. Due to the relatively large leakage current in the samples, only low field electric hysteresis loops were obtained. The samples are highly conductive at room temperature and only partial reversal of the polarization takes place, quite similar to that observed by Pradhan et al. [26]. The relatively high conductivity of BiFeO_3 is known to be attributed to the variable oxidation states of Fe ions (Fe^{2+} to Fe^{3+}), which require oxygen vacancies for charge compensation. Also during synthesis, the slow heating rate and long sintering time will enable the equilibrium concentration of the oxygen vacancies at high temperature to be reached and will result in the high oxygen vacancy concentration in the synthesized product. So the presence of Fe^{2+} ions and oxygen deficiency leads to high conductivity. No saturated polarization hysteresis loop has been observed for all samples at room temperature under the applied field due to high conductivity of the samples. It is striking that only a La substitution can dramatically change the electric polarization behavior, although the remnant polarization is still far less than the expected value of bulk BiFeO_3 samples ($95\text{ }\mu\text{C}/\text{cm}^2$) predicted by theory [30].

4. Conclusions

In summary, La-substituted multiferroic BiFeO_3 ceramic [$\text{Bi}_{1-x}\text{La}_x\text{FeO}_3$ ($x = 0.0, 0.05, 0.10, 0.15, 0.20, 0.25$)] were synthesized using solution combustion method. La substitution

at Bi site eliminated the small impurity phase of BiFeO_3 and stabilized the crystal structure. Both dielectric constant and dielectric loss for samples $x = 0.20, 0.25$ are almost constant and exhibited lowest dielectric loss close to 0.1 (10 KHz to 1 MHz) and the resistivity of $\text{Bi}_{1-x}\text{La}_x\text{FeO}_3$ samples reaches a maximum value of 10^9 ohm-cm , which is about three times higher than that for pure BiFeO_3 . Due to the relatively large leakage current in the samples, only low field electric hysteresis loops were obtained. It is inferred that La doped BiFeO_3 , or more complicated doped BiFeO_3 based on La doping, will have great potential for practical application in electronic devices and various sensors due to the capability of generating a magnetization/electric polarization by an electric/magnetic field.

Acknowledgments

Research facilities provided by Dept. of Physics, H.P. University, Shimla, SAIF Chandigarh are highly acknowledged.

References

- [1] W. Eerenstein, N.D. Mathur, J.F. Scott, Multiferroic and magnetoelectric materials, *Nature* 442 (2006) 759–765.
- [2] M. Li, M. Ning, Y. Ma, Q. Wu, C.K. Ong, Room temperature ferroelectric, ferromagnetic and magnetoelectric properties of Ba-doped BiFeO_3 thin films, *J. Phys. D* 40 (2007) 1603–1607.
- [3] S. Dong, J.-F. Li, D. Viehland, Ultrahigh magnetic field sensitivity in laminates of TERFENOL-D and $\text{Pb}(\text{Mg}_{1/3}\text{Nb}_{2/3})\text{O}_3$ – PbTiO_3 crystals, *Appl. Phys. Lett.* 83 (2003) 2265–2267.
- [4] S. Dong, J. Zhai, J.F. Li, D. Viehland, M.I. Bichurin, Magnetoelectric gyration effect in $\text{Tb}_{1-x}\text{Dy}_x\text{Fe}_{2-y}/\text{Pb}(\text{Zr}, \text{Ti})\text{O}_3$ laminated composites at the electromechanical resonance, *Appl. Phys. Lett.* 89 (2006) 243512–243514.
- [5] W.M. Zhu, Z.-G. Ye, Effects of chemical modification on the electrical properties of 0.67BiFeO_3 – 0.33PbTiO_3 ferroelectric ceramics, *Ceram. Int.* 30 (2004) 1435–1442.
- [6] G.A. Smolenskii, I.E. Chupis, Ferroelectromagnets, *Sov. Phys. Usp* 25 (1982) 475–493.
- [7] P. Fischer, M. Polomska, I. Sosnowska, M. Szymanski, Temperature dependence of the crystal and magnetic structures of BiFeO_3 , *J. Phys. C* 13 (1980) 1931–1940.
- [8] S.-W. Cheong, M. Mostovoy, Multiferroics: a magnetic twist for ferroelectricity, *Nat. Mater.* 6 (2007) 13–20.
- [9] N.A. Hill, Why are there so few magnetic ferroelectrics, *J. Phys. Chem. B* 104 (2000) 6694–6709.
- [10] J. Nogues, I.K. Schuller, Exchange bias, *J. Magn. Magn. Mater.* 192 (1999) 203–232.
- [11] Y.P. Wang, L. Zhou, M.F. Zhang, X.Y. Chen, J.-M. Liu, Z.G. Liu, Room-temperature saturated ferroelectric polarization in BiFeO_3 ceramics synthesized by rapid liquid phase sintering, *Appl. Phys. Lett.* 84 (2004) 1731–1733.
- [12] Q.H. Jiang, J. Ma, Y.H. Lin, C.-W. Nan, Z. Shi, Z.J. Shen, Multiferroic properties of $\text{Bi}_{0.87}\text{La}_{0.05}\text{Tb}_{0.08}\text{FeO}_3$ ceramics prepared by spark plasma sintering, *Appl. Phys. Lett.* 91 (2007) 022914–022916.
- [13] G.L. Yuan, S.W. Or, Enhanced piezoelectric and pyroelectric effects in single-phase multiferroic $\text{Bi}_{1-x}\text{Nd}_x\text{FeO}_3$ ($x = 0–0.15$) ceramics, *Appl. Phys. Lett.* 88 (2006) 062905–062907.
- [14] V.R. Palkar, D.C. Kundaliya, S.K. Malik, S. Bhattacharya, Magnetoelectricity at room temperature in the $\text{Bi}_{0.9-x}\text{Tb}_x\text{La}_{0.1}\text{FeO}_3$ system, *Phys. Rev. B* 69 (2004) 212102–212104.

- [15] K. Sen, S. Thakur, K. Singh, A. Gautam, M. Singh, Room-temperature magnetic studies of La-modified BiFeO₃ ceramic, *Mater. Lett.* 65 (2011) 1963–1965.
- [16] A. Gautam, K. Singh, K. Sen, R.K. Kotnala, M. Singh, Crystal structure and magnetic property of Nd doped BiFeO₃ nanocrystallites, *Mater. Lett.* 65 (2011) 591–594.
- [17] A. Srinivas, D.-W. Kim, K.S. Hong, S.V. Suryanarayana, Observation of ferroelectromagnetic nature in rare-earth-substituted bismuth iron titanate, *Appl. Phys. Lett.* 83 (2003) 2217–2219.
- [18] N. Wang, J. Cheng, A. Pyatakov, A.K. Zvezdin, J.F. Li, L.E. Cross, D. Viehland, Multiferroic properties of modified BiFeO₃–PbTiO₃-based ceramics: random-field induced release of latent magnetization and polarization, *Phys. Rev. B* 72 (2005) 104434–104438.
- [19] S.R. Das, R.N.P. Choudhary, P. Bhattacharya, R.S. Katiyar, P. Dutta, A. Manivannan, M.S. Seehra, Structural and multiferroic properties of La-modified BiFeO₃ ceramics, *J. Appl. Phys.* 101 (2007) 034104–034110.
- [20] C.T. Munoz, J.-P. Rivera, A. Bezinges, A. Monnier, H. Schmid, Measurement of the quadratic magnetoelectric effect on single crystalline BiFeO₃, *Japan J. Appl. Phys. Suppl.* 24 (1985) 1051–1053.
- [21] J.R. Teague, R. Gerson, W.J. James, Dielectric hysteresis in single crystal BiFeO₃, *Solid State Commun.* 8 (1970) 1073–1074.
- [22] B.D. Cullity, *Elements of X-ray Diffraction*, 2nd ed., Addison-Wesley, Reading, MA, 1978.
- [23] F. Chang, N. Zhang, F. Yang, S. Wang, G. Song, Effect of Cr substitution on the structure and electrical properties of BiFeO₃ ceramics, *J. Phys. D* 40 (2007) 7799–7803.
- [24] J.C. Maxwell, *Electricity and Magnetism*, vol. 3, Oxford University Press, London, 1958, 328.
- [25] C.G. Koops, On the dispersion of resistivity and dielectric constant of some semiconductors at audio frequencies, *Phys. Rev.* 83 (1951) 121–124.
- [26] A.K. Pradhan, K. Zhang, D. Hunter, J.B. Dadson, G.B. Loutts, P. Bhattacharya, R. Katiyar, J. Zhang, D.J. Sellmyer, U.N. Roy, Y. Cui, A. Burger, Magnetic and electrical properties of single-phase multiferroic BiFeO₃, *J. Appl. Phys.* 97 (2005) 093903–093906.
- [27] J.K. Kim, S.S. Kim, W.-J. Kim, Sol–gel synthesis and properties of multiferroic BiFeO₃, *Mater. Lett.* 59 (2005) 4006–4009.
- [28] M.M. Kumar, V.R. Palkar, K. Srinivas, S.V. Suryanarayana, Ferroelectricity in a pure BiFeO₃ ceramics, *Appl. Phys. Lett.* 76 (2000) 2764–2766.
- [29] V.R. Palkar, J. John, R. Pinto, Observation of saturated polarization and dielectric anomaly in magnetoelectric BiFeO₃ thin films, *Appl. Phys. Lett.* 80 (2002) 1628–1630.
- [30] P. Baettig, C. Ederer, N.A. Spaldin, First principles study of the multiferroic BiFeO₃, Bi₂FeCrO₆ and BiCrO₃: structure, polarization, and magnetic ordering temperature, *Phys. Rev. B* 72 (2005) 214105–214112.